

Spatial statistics and image analysis. Lecture 10

Mats Rudemo

May 5, 2020

Today's lecture will cover:

Tracking diffusing particles

FRAP (Fluorescence Recovery After Photobleaching)

Estimation of particle concentration from single particle tracking

Estimation of particle concentration from particle count time series

Tracking a single diffusing particle

Let X_i denote the position at time $i\Delta t$, $i = 0, 1, \dots, K$, of a diffusing particle in d -dimensional space, where $d = 1, 2$ or 3 ,

$$X_i = X_{i-1} + \Delta G_i, \quad (1)$$

where ΔG_i are independent d -dimensional normal vectors with a mean vector with all components zero and a covariance matrix

$$C(\Delta G_i) = 2D\Delta t I, \quad (2)$$

where D is the diffusion coefficient and I is the d -dimensional unit matrix.

In each dimension the diffusing particle has a normally distributed increment with mean zero and variance $2D\Delta t$

Increments in different dimensions and at different time-points are independent.

Let $\|x\|$ denote the Euclidean norm, $\|x\|^2 = \sum_j x_j^2$

$$\mathbf{E}\left(\sum_{i=1}^K \|\Delta G_i\|^2\right) = 2dD\Delta t K \quad (3)$$

It follows that

$$\hat{D} = \frac{1}{2d\Delta t K} \sum_{i=1}^K \|\Delta G_i\|^2 \quad (4)$$

is an unbiased estimate of the diffusion coefficient D .

We can also obtain a confidence interval for D

Fluorescence recovery after photobleaching (FRAP)

FRAP is a method for analyzing diffusion which can be applied to the study of possibly heterogenous materials with locally varying diffusion coefficients.

We give here a pixel-based likelihood framework for FRAP.

In FRAP the diffusion coefficient of fluorescent molecules is determined locally in a confocal microscope.

Fluorescent molecules are bleached and deactivated in a vertical cylinder by a high intensity laser pulse of short duration. The result is a decreased fluorescence in the bleached volume, see the upper left image in Figure 1

The sequence of images in Figure 1 shows the evolution of fluorescence in a horizontal 2D area corresponding to a thin volume extending a short distance in the vertical direction.

From the image sequence we see how fluorescence is recovering due to the fact that unbleached molecules diffuse into and bleached molecules diffuse out of the deactivated volume.

The recovery is clearly seen in Figure 1 and even more clearly in Figure 2.

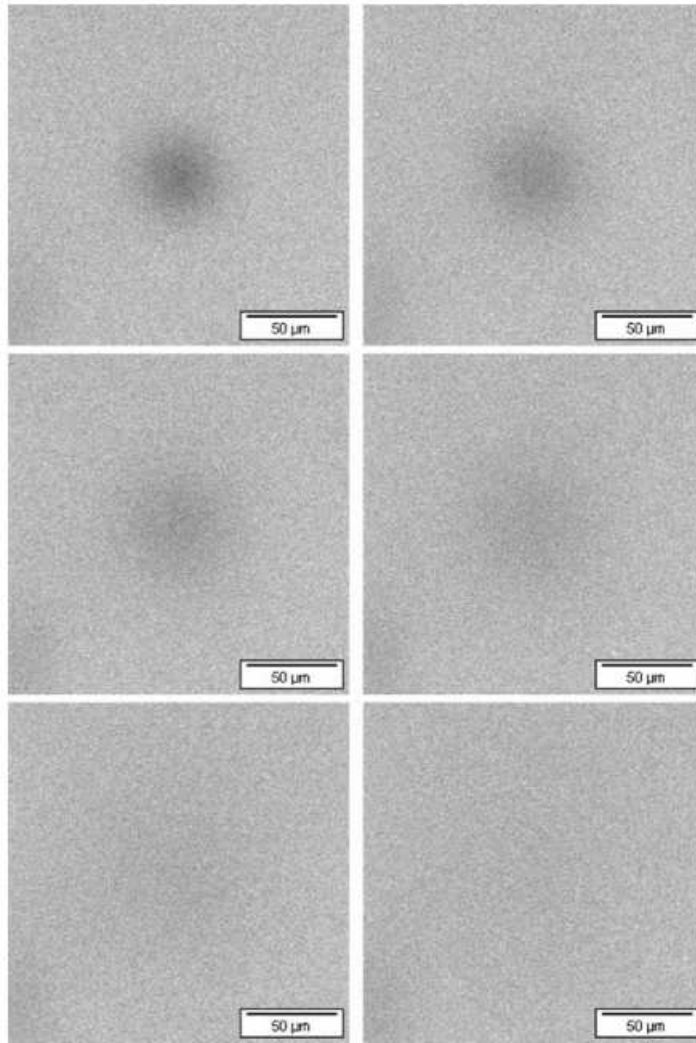


Figure 1: Plots of images from the first photobleaching series with 256 x 256 pixels described in Table 1. The left top image is the first after bleaching, then follows images about 1 s, 2 s, 4 s, 8 s and 16 s later.

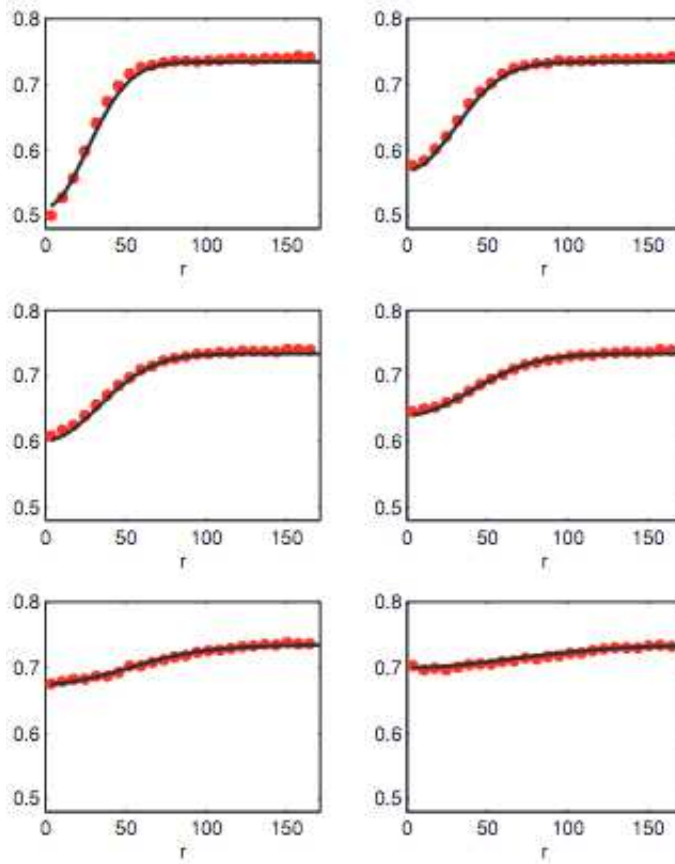


Figure 2: Plots of fitted concentration and pixel values, averaged over pixels with equal distances to the bleaching centre, as a function of distance r to the bleaching centre for the same series as shown in Figure 1. The left top image is the first after bleaching, then follows images about 1 s, 2 s, 4 s, 8 s and 16 s later.

The observed pixel intensity in the images will be modelled by a combination of a solution to the diffusion equation and an assumption of independent normally distributed errors.

The diffusion of fluorochromes is supposed to follow the diffusion equation (similar to the heat equation)

$$\frac{\partial C}{\partial t} = D \left(\frac{\partial^2 C}{\partial x^2} + \frac{\partial^2 C}{\partial y^2} + \frac{\partial^2 C}{\partial z^2} \right), \quad (5)$$

where C is the concentration of unbleached fluorochromes and D is the diffusion coefficient.

Regard a rotationally symmetric bleached region. Assume that there is no net diffusion in the z -direction and that the fluorochromes are initially uniformly distributed.

With polar coordinates the diffusion equation can be written

$$\frac{\partial C}{\partial t} = D \left(\frac{1}{r} \frac{\partial C}{\partial r} + \frac{\partial^2 C}{\partial r^2} \right), \quad (6)$$

where r is the distance from the centre of the bleached region.

Let $C_0(r)$ denote the fluorochrome concentration at time zero (immediately after the high intensity pulse)

Let $I_0(x) = (1/\pi) \int_0^\pi \exp(-x \cos t) dt$ denote the modified Bessel function of order zero. The solution of equation (6) can be written on the form

$$C(r, t) = \frac{1}{2Dt} \exp\left(-\frac{r^2}{4Dt}\right) \int_0^\infty u C_0(u) I_0\left(\frac{ru}{2Dt}\right) \exp\left(-\frac{u^2}{4Dt}\right) du. \quad (7)$$

If we would have complete bleaching the intensity profile immediately after bleaching would be described by an inverse top hat function. However, the bleaching is not complete and diffusion starts directly to blur this profile

In Figures 1 and 2 we see a profile rather different from a top hat. We assume that the initial profile is an approximately Gaussian profile, and suppose that the initial concentration has the form

$$C_0(r) = a_0 - \frac{a_1}{r_0^2} \exp\left(-\frac{r^2}{r_0^2}\right) du. \quad (8)$$

Then the solution of equation (6) with the initial condition $C(0, r) = C_0(r)$ simplifies to

$$C(r, t) = a_0 - \frac{a_1}{4Dt + r_0^2} \exp\left(-\frac{r^2}{4Dt + r_0^2}\right) du. \quad (9)$$

Let $p(i, t)$ denote the observed intensity at time t at pixel i with distance r_i to the centre of the bleached region. We assume that except for additive random noise the pixel intensity is proportional to the fluorochrome concentration $C(r_i, t)$.

Assume further that pixel-wise the noise is normal with mean zero and variance σ^2 with independence between different pixels and different times.

Let S denote the set of pixels and T the set of times regarded. Assume that the pixel-values $p(i, t), i \in S, t \in T$, are independent with probability density

$$f(p(i, t); a_0, a_1, D, r_0, \sigma^2) = \frac{1}{\sqrt{2\pi\sigma^2}} \exp\left(-\frac{(p(i, t) - C(r_i, t))^2}{2\sigma^2}\right). \quad (10)$$

The likelihood function is the joint probability density for all pixels and all times, and due to independence it is

$$L(\theta) = \prod_{t \in T} \prod_{i \in S} \frac{1}{\sqrt{2\pi\sigma^2}} \exp\left(-\frac{(p(i, t) - C(r_i, t))^2}{2\sigma^2}\right), \quad (11)$$

where θ is the parameter vector $\theta = (a_0, a_1, D, r_0, \sigma^2)$.

The log-likelihood $\ell(\theta) = \log L(\theta)$ is then

$$\ell(\theta) = \frac{|T||S|}{2} \log(2\pi\sigma^2) - \frac{1}{2\sigma^2} \sum_{t \in T} \sum_{i \in S} (p(i, t) - C(r_i, t))^2, \quad (12)$$

and it is maximized with respect to the parameter vector θ to find the ml estimates, the most likely parameter values given the observed images.

Likelihood theory allows computation of parameter estimates together with corresponding standard errors. The parameter estimates are approximately multivariate normally distributed with a covariance matrix that is the inverse of the observed information matrix.

The entry in row j and column k of the observed information matrix is

$$-\frac{\partial^2}{\partial\theta_j\partial\theta_k}\ell(\theta), \quad (13)$$

evaluated at $\theta = \hat{\theta}$, where $\hat{\theta}$ is the ml estimate of θ . If the coordinates of the centre of the bleached disk are unknown there will be two extra parameters in the likelihood.

In Table 1 results from experiments with a Sodium Fluorescein probe in polyethylene glycol are reported. Two series of experiments with respectively 128×128 pixel images and 256 x 256 pixel images were performed, and in each series four replicates with differently placed bleaching centres were used. Results from the experiments are shown in and for one of the replicates in more detail in Figures 1 and 2.

Table 1: Results from an experiment with two replicate series. For the first four replicates (with 128×128 pixels) 48 images were used and for the last four replicates (with 256 x 256 pixels) 18 images were used. The columns D and s show diffusion coefficients and standard errors estimated by maximum likelihood, while \bar{D} and s_{repl} show averages and standard deviation from the replicate series.

Replicate	No of pixels	D ($\mu m^2/s$)	s ($\mu m^2/s$)	\bar{D} ($\mu m^2/s$)	s_{repl} ($\mu m^2/s$)
1	128×128	64.3	0.8		
2	128×128	60.1	0.8		
3	128×128	61.1	0.8		
4	128×128	59.6	0.8	61.3	2.1
1	256×256	61.0	0.5		
2	256×256	61.8	0.5		
3	256×256	60.8	0.4		
4	256×256	63.8	0.5	61.8	1.4

As a check of the FRAP results given in Table 1 a corresponding NMR diffusometry experiment was performed. It gave an estimated diffusion coefficient of 62.0 $\mu m^2/s$ with a standard error of 1.9 $\mu m^2/s$, which is well in line with the results in Table 1.

Estimation of particle concentration from single-particle tracking

Nano-sized fluorescent particles observed in a microscope can typically be detected in a rather thin rectangular box such as shown in Figure 3.

To determine particle concentration we need to know the dimensions of the detection region. The extension in the horizontal directions can usually be determined in a straightforward way from the microscope field of view.

But the size in the vertical direction is much more difficult to measure as it depends on a number of factors such as the particle detection algorithm and the brightness of the observed particles. Such properties are not fixed but can vary considerably between experiments.

This problem is analyzed in Rödning et al. (2008) and the vertical dimension is estimated from the trajectory length distribution.

Assume that the detection region thickness is considerably smaller than the horizontal dimensions which means that particles typically enter and leave the detection region by moving upwards or downwards.

The trajectory length distribution is then essentially determined by the detection region thickness. Roughly, short trajectory lengths indicate a small thickness.

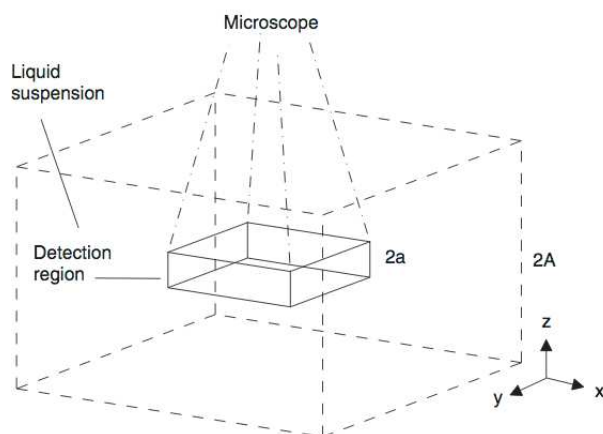


Figure 3: A microscope detection region modeled as a rectangular box centred in the liquid suspension where particles move. Particles outside the detection region cannot be observed. The tracking depth is $2a$ and the thickness of the suspension is $2A$.

Assume that we observe a particle at positions X_i at K equidistant time-points $t_i = i\Delta t, i = 1, \dots, K$, typically corresponding to K consecutive frames in a video sequence.

The particle enters the detection region at time t_1 and leaves it after K observed positions. The particle moves in 3D but we simplify and consider only the motion in 1D, in the z -direction.

Assume that the particle enters and leaves the detection region from above or below – a good approximation when the vertical dimension $2a$ of the detection region is much smaller than the horizontal dimensions. Assume also that the detection region thickness $2a$ is much smaller than the thickness $2A$ of the liquid suspension volume.

Considering only 1D diffusion in the z -direction we assume that initially the particle position is uniformly distributed in the interval $[-A, A]$ and a particle outside the detection region is assumed to be uniformly distributed over $[-A, -a] \cup [a, A]$.

Let $f(z)$ denote the probability density of the position of a particle that has just entered the detection region. One can then show that $f(z) = 0$ for $|z| > a$ and

$$f(z) = \frac{h(z)}{\int_{-a}^a h(z) dz}, \quad z \in [-a, a], \quad (14)$$

where

$$h(z) = \frac{1}{2(A-a)} \left[\Phi\left(\frac{z+A}{\sqrt{2D\Delta t}}\right) - \Phi\left(\frac{z+a}{\sqrt{2D\Delta t}}\right) + \Phi\left(\frac{z-a}{\sqrt{2D\Delta t}}\right) - \Phi\left(\frac{z-A}{\sqrt{2D\Delta t}}\right) \right] \quad (15)$$

and Φ denotes the standard normal cumulative distribution function.

Let Z_k denote the position of a particle and let f_k denote the non-normalized density of the particle position after k steps assuming that $K \geq k$, more precisely $f_k(z) = d/dz[P(Z_k \leq z \text{ and } K \geq k)]$, for $k \geq 1$.

By definition $f_k(z)$ is zero outside $[-a, a]$. For the first position of the particle in the detection region we have $f_1 = f$ given by (14). To compute the probability density of the particle after step 2, f_1 is convolved with the Gaussian propagator

$$G(z) = \frac{1}{\sqrt{2D\Delta t}} \phi\left(\frac{z}{\sqrt{2D\Delta t}}\right), \quad (16)$$

where ϕ is the density of a standardized normal variable. Since we assume that the particle stays in the detection region K steps it cannot be outside the interval $[-a, a]$ and the density has to be truncated.

Generally the density f_k can be recursively computed from f_{k-1} according to

$$f_k(z) = \begin{cases} \int_{-\infty}^{\infty} f_{k-1}(z_0)G(z - z_0) dz_0, & z \in [-a, a], \\ 0, & z \notin [-a, a]. \end{cases} \quad (17)$$

Computation of f_k for $k > 1$ cannot be performed analytically, but there is a fast numerical scheme with probability densities approximated by translates of a Gaussian kernel.

In Figure 4 the computation of the sequence of densities $f_k, k \geq 1$ is illustrated.

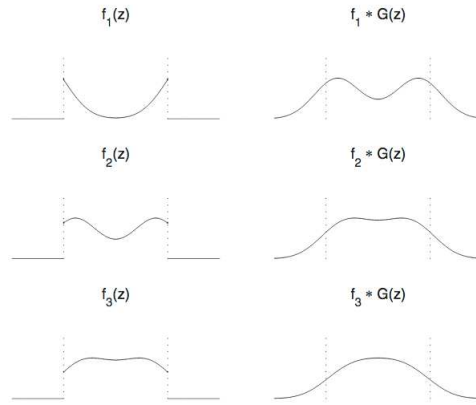


Figure 4: Illustration of the procedure for computing the trajectory length distribution. Here $f_1(z)$ is the probability density of a particle that has just entered the detection region according to equation (14). Truncation outside of $[-a, a]$ of the convolution $f_1 * G(z)$ yields the non-normalized density $f_2(z)$ which integrates to the probability that the particle still remains in the detection region for a second sampling point, and so forth.

The probability that a particle stays in the detection region for at most k consecutive steps is

$$P_a(K \leq k) = 1 - \int_{-a}^a f_{k+1}(z) dz, \quad (18)$$

where the dependence on a is emphasized. The probability distribution for the trajectory length is then obtained from

$$P_a(K = k) = P_a(K \leq k) - P_a(K \leq k - 1). \quad (19)$$

Suppose now that we have observed an ensemble of identical particles with known diffusion coefficient. The assumption of known (or well estimated) diffusion coefficient is reasonable as it can readily be estimated from the particle trajectories, compare (4).

Let us consider trajectories with length $K \geq k_{min}$. It is typical to impose a lower threshold like $K \geq 3$ or $K \geq 4$ for the trajectory length as shorter trajectories are more likely to be false positives. Let N_k denote the number of observed trajectories of length k . Then the log-likelihood function is

$$\ell(a) = \sum_{k \geq k_{min}} N_k \log P_a(K = k | K \geq k_{min}), \quad (20)$$

where

$$P_a(K = k | K \geq k_{min}) = \frac{P_a(K = k)}{P_a(K \geq k_{min})} \quad (21)$$

and $P_a(K \geq k_{min})$ is computed from (18). The maximum likelihood estimate \hat{a} is the a -value that maximizes $\ell(a)$ in (20).

After having estimated the tracking depth a it is possible to estimate the particle concentration. Let \bar{N} denote the mean number of particles per video frame. A suitable point estimator of the particle concentration c is

$$\hat{c} = \frac{\bar{N}}{8\hat{a}a_x a_y 10^{-12}} \text{ particles/ml}, \quad (22)$$

where $2a_x$ and $2a_y$ are the lateral sizes in μm of the detection region.

We can estimate \bar{N} by counting trajectories as follows. Let n be the number of frames, and let N_k as earlier be the number of observed trajectories of length k . The number of observed particle positions is the sum of all trajectory lengths. Dividing by the number of frames we get an estimate of the mean number of particles per frame, and we estimate \bar{N} by

$$\bar{N} = \frac{1}{\hat{p}_{obs}} \frac{1}{n} \sum_{k \geq k_{min}} k N_k. \quad (23)$$

The factor \hat{p}_{obs} corrects for underestimation of the concentration due to discarding trajectories with length $k < k_{min}$,

$$\hat{p}_{obs} = \frac{\sum_{k \geq k_{min}} k P_{\hat{a}}(K = k)}{\sum_{k \geq 1} k P_{\hat{a}}(K = k)}. \quad (24)$$

With this correction factor the estimate \bar{N} in (23) becomes approximately unbiased.

The standard error of the concentration estimate can be assessed by bootstrapping. It is here suitable to perform the bootstrapping on video level, since videos are (approximately) independent.

Thus B bootstrap samples are obtained by sampling B times with replacement from the set of videos, and from each sample the concentration estimates $\hat{c}_1, \dots, \hat{c}_B$ are computed according to (22). This gives an approximate standard deviation estimate

$$\sigma_{\hat{c}} = \left(\frac{1}{B-1} \sum_{i=1}^B (\hat{c}_i - c_{mean})^2 \right)^{1/2}, \quad (25)$$

where c_{mean} is the mean of the bootstrap estimates. This method relies on that the videos are approximately equally long and independent.

The simulation study briefly described below, leads to the conclusion that the tracking depth and the concentration estimates are approximately unbiased and that bootstrap errors for $B = 50$ are quite close to the actual standard errors.

In the simulation study particles were moving according to 3D random walk with time increments Δt and independent zero mean normally distributed increments with variance $2D\Delta t$ in all three dimensions. Particles moved in a cube with side length $2A = 40 \mu m$, compare Figure 3, with periodic boundary conditions.

Particle trajectories were recorded when particles entered the detection region. In the study three different diffusion coefficients, $D = 1 \mu\text{m}^2/\text{s}$, $D = 2 \mu\text{m}^2/\text{s}$, and $D = 5 \mu\text{m}^2/\text{s}$, and a series of values for the detection region thickness from 0.1 to $2 \mu\text{m}$ were used. The concentration of particles was $c = 10^9$ particles/ml. For each combination of diffusion coefficient and detection region thickness 20 000 simulations were performed and the mean obtained estimates of a and c are shown in Figure 5.

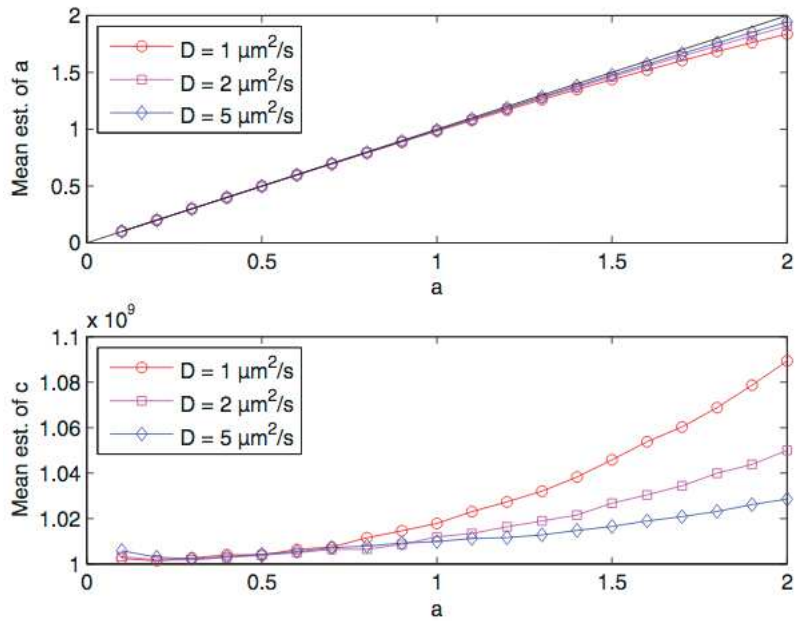


Figure 5: Simulation study of the tracking depth parameter a (upper) and the concentration c (lower). Mean estimates are shown for $D = 1 \mu\text{m}^2/\text{s}$ (red circles), for $D = 2 \mu\text{m}^2/\text{s}$ (magenta squares), and for $D = 5 \mu\text{m}^2/\text{s}$ (blue diamonds) as functions of the true value of a . The true value of a is given by the black solid line. The true concentration of particles was $c = 10^9$ particles/ml. The increasing bias (negative for a and positive for c) for increasing a is due to the 1D approximation in the model for the trajectory length distribution.

In addition to the results from simulations, results from experiments with $0.19\text{-}\mu\text{m}$ and $0.52\text{-}\mu\text{m}$ particles are also reported in (?). In Figure 6 we see concentration estimates for 5 dilutions with the $0.19\text{-}\mu\text{m}$ particles. Estimated 95% confidence intervals obtained by bootstrapping for each dilution are also shown.

Ideally the concentration estimates should fall on the solid straight line shown. However, this line is not perfectly known as there are some uncertainties of the size of the particles. Mean particle diameter was estimated by use of light scattering and was found to be $0.207\ \mu\text{m}$ with a standard deviation of $0.008\ \mu\text{m}$. From this a 95% confidence interval for the solid line is obtained and shown in Figure 6.

From Figures 5 and 6 we see that the method described performs well both for simulated and experimental data.

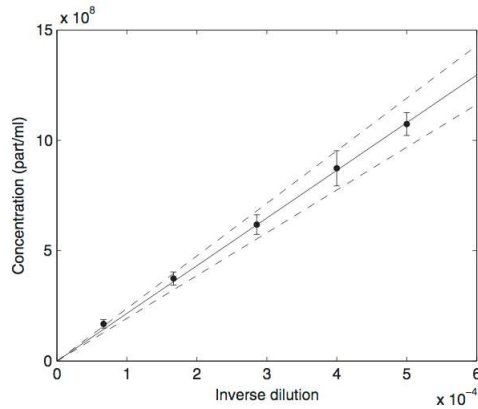


Figure 6: Experimental results with estimated concentrations for different dilutions of $0.19\text{-}\mu\text{m}$ particles with estimated 95% confidence intervals. The concentration as estimated from the stock-solution concentration (solid line) and estimated 95% confidence intervals (dashed lines) are also shown.

Estimation of particle concentration from particle count time series

The method for estimation of particle concentration discussed in the previous section requires particle tracking, that is pairing particles from one frame to the following frame. This may be difficult for fast particles and high concentrations. We will now describe a method which only requires counting the number of particles in each frame but no tracking of the individual particles.

In Figure 7 we see an experimentally observed count process with the number of particles varying between about 18 and 37 particles. Such a process of particle counts we call a Smoluchowski process in honour of the Polish physicist M. von Smoluchowski who in 1906 developed an alternative to Einstein's description from 1905 of Brownian motion.

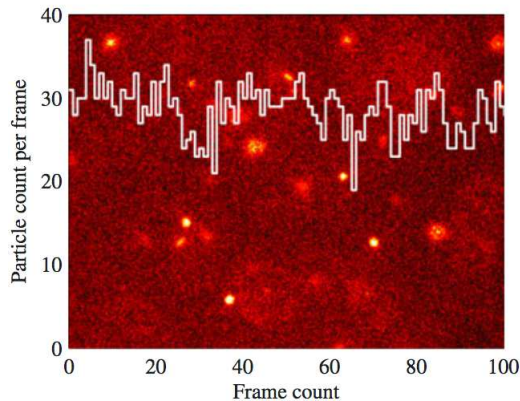


Figure 7: An example of an experimentally observed Smoluchowski process obtained by counting liposomes in whole blood, superimposed over a sample frame from the raw image data, compare Braeckmans et al. 2010.

We will assume that particles move in and out of a microscope detection region of the type shown in Figure 3. In this section we will call the lateral dimensions of the detection region $2a_x$ and $2a_y$ and the vertical dimension $2a_z$. Thus $2a$ in Figure 3 corresponds here to $2a_z$.

The number of particles in a sequence of frames varies as illustrated in Figure 8.

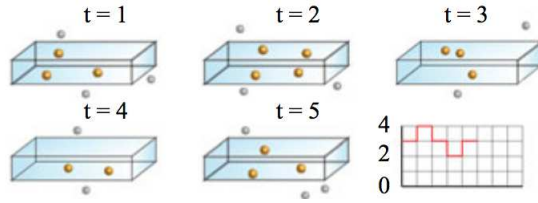


Figure 8: Illustration of a Smoluchowski process. Diffusing particles reside both inside (yellow) and outside (grey) the detection region. Particles moving in and out of the detection region and the number of detected particles is fluctuating, forming a random time series.

Let us now describe an approximate Markov statistical model for the Smoluchowski process. We assume that particles move independently of each other according to a Brownian motion with independent increments in all three dimensions with mean zero and variance $2D\Delta t$, where Δt is the interval between observations (frames).

Let $X_n, n = 1, \dots, N$, denote the number of particles observed in the n th frame. Then

$$X_{n+1} = X_n - O_n + I_n, \quad (26)$$

where O_n is the number of particles, out of the X_n particles initially present, exiting the detection region, and I_n is the number of particles entering that region, between the two observations X_n and X_{n+1} .

We shall assume that regardless of observation up to (and including) X_n the random variable I_n is Poisson distributed with a parameter λ , that is,

$$\Pr(I_n = k | X_1, \dots, X_n) = \frac{\lambda^k}{k!} e^{-\lambda}. \quad (27)$$

Another assumption, which we shall make, is that given observations up to (and including) X_n , the random variable O_n is binomially distributed with probability-parameter μ , more precisely, that

$$\Pr(O_n = j | X_1, \dots, X_n) = \binom{X_n}{j} \mu^j (1 - \mu)^{X_n - j}. \quad (28)$$

Based on these assumptions we approximate the distribution of the process of particle counts $(X_n, n \geq 1)$ with a Markov model with transition probabilities $p_{ij} = \Pr(X_{n+1} = j | X_n = i)$ given by

$$p_{ij}(\lambda, \mu) = e^{-\lambda} \sum_{k=\max(0, j-i)}^j \frac{\lambda^k}{k!} \binom{i}{i-j+k} \mu^{i-j+k} (1 - \mu)^{j-k}. \quad (29)$$

One can show that a Markov chain with transition probabilities given by (29) has a stationary distribution which is a Poisson distribution with parameter λ/μ , that is

$$\Pr(X_n = k) = \pi_k = \frac{(\lambda/\mu)^k e^{-\lambda/\mu}}{k!}. \quad (30)$$

Given the Markov assumption the joint distribution of particle counts X_1, \dots, X_N can be written

$$\Pr(X_1 = x_1, \dots, X_N = x_N) = \Pr(X_1 = x_1) \prod_{k=2}^N \Pr(X_k = x_k | X_{k-1} = x_{k-1}). \quad (31)$$

For a realization x_1, \dots, x_N we obtain a log-likelihood function $\ell(\lambda, \mu) = \ell(\lambda, \mu | x_1, \dots, x_N)$ given by

$$\ell(\lambda, \mu) = \log \frac{(\lambda/\mu)^{x_1} e^{-\lambda/\mu}}{x_1!} + \sum_{i,j} N_{ij} \log p_{ij}(\lambda, \mu), \quad (32)$$

where N_{ij} is the number of transitions from state i to state j . We obtain the maximum likelihood estimates $\hat{\lambda}$ and $\hat{\mu}$ by maximizing the log-likelihood $\ell(\lambda, \mu)$. For estimation of the lateral dimension parameter a_z it turns out that the crucial parameter is μ .

The parameter μ may be interpreted as the probability that a particle uniformly distributed in the detection region exits this region in a time interval of length Δt , compare (28). With this interpretation one can show that

$$\mu = \mu(a_z) = 1 - F(a_x, D)F(a_y, D)F(a_z, D), \quad (33)$$

with

$$F(a, D) = \frac{\sqrt{2D\Delta t}}{2a} \left\{ \frac{2a}{\sqrt{2D\Delta t}} \left[2\Phi \left(\frac{2a}{\sqrt{2D\Delta t}} \right) - 1 \right] + 2\phi \left(\frac{2a}{\sqrt{2D\Delta t}} \right) - 2\phi(0) \right\}, \quad (34)$$

where Φ and ϕ denote the distribution function and the probability density of a standardized normal variable. Note that in (33) we write $\mu = \mu(a_z)$ because here a_z is the important unknown parameter.

The lateral dimension parameters a_x and a_y can be measured directly from the microscope geometry and D here needs to be estimated separately, for instance by separate particle tracking. Let us also note that in order to obtain valid standard errors and confidence intervals it is suitable, to use bootstrapping on the 'video level'.

To validate the suggested method both simulations and experiments were used. In the simulations a predetermined number of particles were allowed to diffuse in three dimensions in rectangular box, as the large box in Figure 3, with periodic boundary conditions. Three different diffusion coefficients, $D = 1$, $D = 2$ and $D = 5 \mu\text{m}^2\text{s}^{-1}$, and 20 different a_z -values ranging between 0.1 and 2 μm were used.

The resulting estimates of the detection depth parameter a_z and the concentration are shown in Figure 9. From the figure we see that the method performs very well except for some minor bias for small a_z -values.

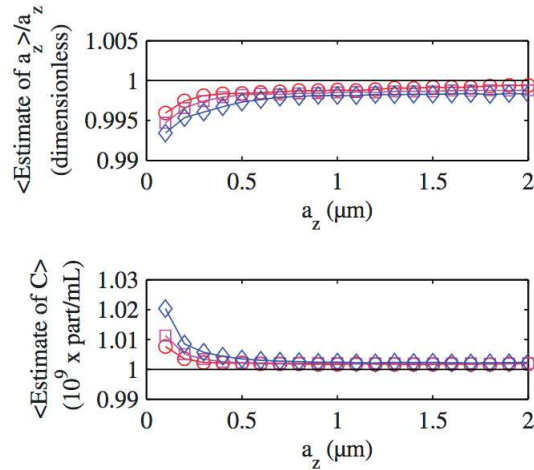


Figure 9: Simulation study of estimation of the detection depth parameter a_z and the concentration estimate C . For $D = 1 \mu\text{m}^2\text{s}^{-1}$ (red circles), $D = 2 \mu\text{m}^2\text{s}^{-1}$ (magenta squares) and $D = 5 \mu\text{m}^2\text{s}^{-1}$ (blue diamonds) the mean estimates of a_z (divided by the true value of a_z) and C are shown as functions of the true value of a_z . The mean estimates were computed from 10^6 simulations for each data point, and the true concentration of particles was $C = 10^9$ particle mL^{-1} .

To experimentally verify the method suggested two experiments with fluorescent polymer nanospheres with diameter $0.2\ \mu\text{m}$ and $0.5\ \mu\text{m}$ were performed. We will here show the results for the smaller diameter. A water dispersion of the particles was diluted by a factor of 1900, 2400, 3400, 5800 and 14800. The theoretical concentration of particles in particles mL^{-1} can be estimated from

$$C_{\text{theoretical}} = \frac{6 \times 10^{10} \times S \rho_L}{\pi \rho_S d^3}, \quad (35)$$

where $S = 1$ is the weight percent of solids, with a relative standard deviation of 5%, $\rho_L = 1.00\ \text{g cm}^{-3}$ is the density of the suspension, $\rho_S = 1.05\ \text{g cm}^{-3}$ is the density of the solid particles (all values according to the manufacturer).

Further, using dynamic light scattering the diameter of the particles was found to be $d = 0.207 \mu\text{m}$ with a standard deviation of $0.008 \mu\text{m}$ (in correspondence with the manufacturer results for the particular batch of nanospheres). Using the standard error-propagation equation the theoretical particle concentration with standard deviations were found for all dilutions and compared with the results from the method suggested.

The results are shown in Figure 10 and it clear from the figure that an excellent agreement was found between the theoretically and experimentally obtained concentration values.

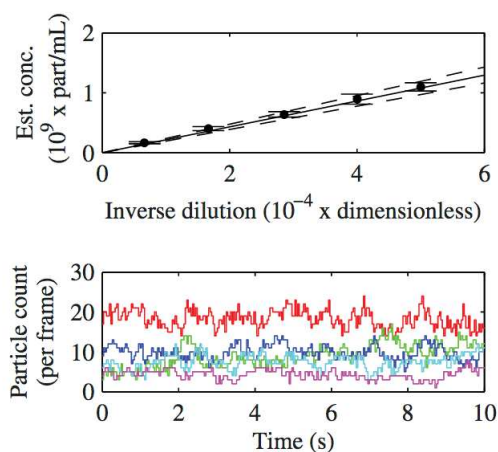


Figure 10: Estimated concentrations from an experiment with different dilutions of $0.2 \mu\text{m}$ particles with estimated 95% confidence intervals ('inverse dilution' is a 'relative concentration'). The concentration as estimated from the stock-solution concentration (solid line) with estimated 95% confidence intervals (dashed lines) is shown (upper). Further, typical examples of the underlying Smoluchowski processes are shown with colours red/green/blue/cyan/magenta in order of of decreasing concentration (lower).